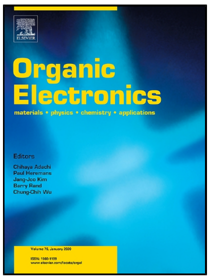

# A Symmetric Nonpolar Blue AIEgen as Nondoped Fluorescent OLED Emitter with Low Efficiency Roll-Off

Nannan Fei, Qiang Wei, Liang Cao, Yongqi Bai, Honglei Ji, Ruixiang Peng, Like Huang, Shiyou Hao, Ziyi Ge

PII: S1566-1199(19)30601-9
DOI: https://doi.org/10.1016/j.orgel.2019.105574
Reference: ORGELE 105574

To appear in: *Organic Electronics*

Received Date: 08 April 2019
Accepted Date: 21 November 2019

Please cite this article as: Nannan Fei, Qiang Wei, Liang Cao, Yongqi Bai, Honglei Ji, Ruixiang Peng, Like Huang, Shiyou Hao, Ziyi Ge, A Symmetric Nonpolar Blue AIEgen as Nondoped Fluorescent OLED Emitter with Low Efficiency Roll-Off, *Organic Electronics* (2019), https://doi.org/10.1016/j.orgel.2019.105574

# A Symmetric Nonpolar Blue AIEgen as Nondoped Fluorescent OLED Emitter with Low Efficiency Roll-Off

Nannan Fei[a,b], Qiang Wei[b*], Liang Cao[b], Yongqi Bai[b], Honglei Ji[b], Ruixiang Peng[b],
Like Huang[b], Shiyou Hao[a*] and Ziyi Ge[b*]

[a] *Xingzhi College, College of Chemistry and Life Sciences, Zhejiang Normal Universtity, Jinhua 321004, P. R. China*
[b] *Ningbo Institute of Materials Technology & Engineering, Chinese Academy Sciences, Ningbo 315201, P. R. China*
*E-mail addresses: weiqiang@nimte.ac.cn; sky54@zjnu.cn; geziyi@nimte.ac.cn*

## Abstract

Blue emitters are necessary for achieving full-color displaying OLEDs, however, most blue emitters show low efficiency, short lifetime or serious efficiency roll-off, hindering the development of OLED techniques. In this research, a nonpolar symmetric aggregation-induced emission (AIE) emitter was designed and constructed through facile steps, with the triphenylamine-end, anthracene-spacer and tetraphenylethene (TPE)-center. This emitter exhibited good thermal stability and aggregation-enhanced emission (AEE) characteristics, based on which non-doped blue OLED device was readily fabricated with the maximum external quantum efficiency (EQE) of 2.7% and also with no efficiency roll-off even at 1000 cd.m$^{-2}$, indicative of high efficiency and good stability as fluorescent emitter.

## Keywords:

aggregation-induced emission; organic light-emitting devices; tetraphenylethene; anthracene; roll-off;

## 1. Introduction

Organic light-emitting devices (OLEDs) have received significant research interests both in academia and industry due to their applications in solid-state lighting and full-color displaying with the evident advantages of low energy cost, high operating voltage, active illumination and full-solid state.[1-4] The OLED emitters, as the core component of the devices, can decide both the performance and the fabricating methods of the OLED device.[5, 6] In order to obtain full-color displaying, the red, green and blue (RGB) emitters are the three primary emitters. However, compared with other two primary emitters, the blue emitters show low efficiency, short lifetime or serious efficiency roll-off, due to their larger band gap and aggregation-caused quenching (ACQ) effects, which strongly limited the development of OLED techniques.[7, 8] Therefore, most current blue OLED devices take advantages of the doping method, however, the doped systems usually suffer from the drawbacks of phase segregation, color aging and poor reproducibility.[9] In contrast to ACQ emitters, the emitters with aggregation-induced emission (AIE) properties, or AIEgens, such as tetraphenylethene(TPE), can overcome the quenching effects in solid state, which are favored to prepare the high-efficient non-doped OLED devices, with the advantages of simplified process and reduced cost in fabrication. [10, 11] On the other hand, anthracene, as a typical polycyclic aromatic hydrocarbon (PAHs), usually serves as building blocks for efficient blue emitters, due to high photoluminescence (PL), ready chemical modification and good thermal stability, but the planar structure of anthracene in aggregated-state tend to form close $\pi$–$\pi$ stacking and further to deteriorate the emitters‘ EL performances.[12, 13]

In previous research, various AIEgen were fabricated with high efficiency as OLED emitters, but many of them have the moieties of strong polarity, which tend to cause efficiency roll-off at high luminescence, due to intra-/intermolecular interactions. Herein, in order to design high efficient and stable blue emitters, we linked the anthraces moiety to the TPE core to suppress its molecular packing, and an important moiety of the commercial triphenylamine (TPA) as the terminal group, due to its nonplanar propreller-shaped to prevent the aggregation of the anthraces and good hole-transporting properties.[14-16] The symmetric TPE emitter can applied in the non-doped blue OLED device with the maixmum external quantum efficiency (EQE) of 2.7%, and the device showed no efficiency roll-off even at 1000 cd.m$^{-2}$.

## 2. Experimental section

### 2.1 General information

All chemicals applied into reaction were received without further purification. Only titanium(IV) chloride was purchased from Alfa Aesar, while all the other chemicals, including N,N-diphenyl-4-(4,4,5,5-tetramethyl-1,3,2-dioxaborolan-2-yl)aniline (CAS No.: 267221-88-5), 9,10-dibromoanthracene ( CAS No. : 523-27-3) and 9-phenyl-9H-carbazol-3-ylboronic acid (CAS No. : 854952-58-2), were supplied by Energy Chemicals.

### 2.2 Synthetic procedures

*1,2-bis(4-bromophenyl)-1,2-diphenylethene* (**TPE-Br**) and*1,2-diphenyl-1,2-bis(4-(4,4,5,5-tetramethyl-1,3,2-dioxaborolan-2-yl)phenyl)ethene* (**TPE-BE**) in this research was synthesized according to previous research.[17] The related data are listed as follows: *1,2-bis(4-bromophenyl)-1,2-diphenylethene* (**TPE-Br**) : $^1$H NMR (400 MHz, $CDCl_3$), $\delta$ (TMS, ppm): 6.87, 6.99, 7.10, 7.20. $^{13}$C NMR (100 MHz, $CDCl_3$), $\delta$ (TMS, ppm): 120.6, 126.9, 127.7, 128.0, 130.8, 131.2, 132.8, 140.2, 142.3, 142.7. ESI-TOF-MS ($C_{26}H_{18}Br_2$): m/z 487.9794 ($M^+$ calculated 487.9775).

*1,2-diphenyl-1,2-bis(4-(4,4,5,5-tetramethyl-1,3,2-dioxaborolan-2-yl)phenyl)ethene* (**TPE-BE**): $^1$H NMR (400 MHz, $CDCl_3$), $\delta$ (TMS, ppm): 1.32, 7.0–7.1, 7.53. $^{13}$C NMR (100 MHz, $CDCl_3$), $\delta$ (TMS, ppm): 25.1, 83.4, 126.7, 127.8, 127.9, 130.9, 131.5, 134.2, 124.3, 141.4, 143.5, 146.9. ESI-TOF-MS ($C_{38}H_{42}B_2O_4$): m/z 584.3314 ($M^+$ calculated 584.3269).

*4-(10-bromoanthracen-9-yl)-N,N-diphenylaniline* (**TPA-An-Br**): A mixture of N,N-diphenyl-4-(4,4,5,5-tetramethyl-1,3,2-dioxaborolan-2-yl)aniline ( CAS : 267221-88-5) (2.02 g, 5.39 mmol) and 9,10-dibromoanthracene ( CAS : 523-27-3) (2.20 g, 6.46 mmol), $Pd(PPh_3)_4$ (0.48 g, 0.42 mmol) and $K_2CO_3$ (9.60 g, 69.7 mmol), were added into a 250 mL two-neck bottle under nitrogen. After then, 150 mL mixed solvent of THF and $H_2O$ (v/v = 4:1) was injected into the bottle, and the mixture was refluxed for 24 h. After cooling to room temperature, the mixture was poured into water and extracted with dichloromethane. The combined organic layers were then dried over anhydrous magnesium sulfate, filtrated, evaporated and finally purifed by silica-gel column chromatography using hexane/dichloromethane as eluent. 2.0g of bright yellow solid **Cz-An-Br** was obtained with yield of 74.2 %. $^1H$ NMR (400 MHz, $CDCl_3$), $\delta$ (TMS, ppm): 8.60, 8.58, 7.81, 7.79, 7.60, 7.58, 7.56, 7.43, 7.41, 7.39, 7.34, 7.32, 7.30, 7.26, 7.25, 7.24, 7.23, 7.09, 7.07, 7.05. $^{13}C$ NMR (100 MHz, $CDCl_3$), $\delta$ (TMS, ppm): 147.80, 147.51, 137.81, 132.06, 131.83, 131.35, 130.40, 129.54, 127.98, 127.59, 127.04, 125.60, 124.91, 123.36, 122.93, 122.70, 77.16. ESI-TOF-MS ($C_{32}H_{22}BrN$): m/z 499.0944 ($M^+$ calculated 499.0936).

*4,4'-(((1,2-diphenylethene-1,2-diyl)bis(4,1-phenylene))bis(anthracene-10,9-diyl))bis (N,N-diphenylaniline) (TPA-An-TPE):* The compound **TPA-An-TPE** was also prepared through Suzuki reaction. In this preparation, **TPE-BE** (1.0 g, 1.75mmol), **TPA-An-Br** (1.370 g, 5.22 mmol), $Pd(PPh_3)_4$ (329 mg, 0.285 mmol) and $K_2CO_3$ (6.55g, 47.4 mmol) were placed into the mixed solvent of THF and water (v/v = 4:1) to reflux for 24 h under nitrogen, and finally 0.32 g of bright yellow solid **TPA-An-TPE** were obtained in the yield of 15.3 %. $^1H$ NMR (400 MHz, $CDCl_3$), $\delta$ (TMS, ppm): 7.86, 7.85, 7.83, 7.81, 7.79, 7.68, 7.45-7.29, 7.28-7.20, 7.10-7.04. $^{13}C$ NMR (100 MHz, $CDCl_3$), $\delta$ (TMS, ppm): 147.85, 147.13, 143.27, 137.43, 132.73, 132.15, 131.51, 131.34, 130.76, 130.03,129.89, 129.40, 127.92, 126.91, 125.21,

124.69, 123.09, 76.70. ESI-TOF-MS **(**$C_{90}H_{62}N_2$**)**: m/z 1170.4915 ($M^+$ calculated 1170.4913).

### 2.3 Device fabrication and characterization

The materials to fabricate OLED devices were purchased from Jinlin Optical and Electronic Materials Co. The Indium-doped tin oxide (ITO) glass sheet (1.2 mm thick, ⩽ 15 Ω/square, transmittance > 90%) was purchased from Nippon Sheet Glass Company, Ltd, and cleaned by a routine cleaning procedure which includes initial manual washed in aqueous detergent, and then sequentially sonication in acetone, isopropanol and ethanol for 30 minutes each. Then, the pre-cleaned ITO glass was moved into an ultraviolet chamber for UV-ozone treatment of 20 minutes. The synthesized emitting material **TPA-An-TPE** were further purified through sublimation at 220 $^{o}$C under the vacuum of $1.5\times10^{-3}$ Pa in the sublimation system (CSe solar ETS-60T-S) before fabricating the OLED devices. The organic layers were deposited consecutively on the pre-cleaned ITO glass substrates in a vacuum chamber ($5\times10^{-4}$ Pa). The deposition rate of all the organic materials was 0.9-1.1Å $S^{-1}$, while that of the LiF was 0.1 Å $S^{-1}$and aluminum was 5 Å $S^{-1}$. The electrical characteristics of the devices were measured with a Keithey 2400 Source meter at the range of 0-15V. The electroluminescence spectra and luminance of the devices were obtained on a PR655 spectrometer in ambient conditions at room temperature.

## 3. Result and discussion

### 3.1 Synthesis of materials

The molecular structure of **TPE-An-TPA** and its synthetic route were illustrated in **Scheme 1**. To be specific, the AIEgen of **TPE-En-TPA** was prepared through Suzuki coupling between the two precursor of TPE-bearing boric acid ether **TPE-BE** and the Br-containing precursor **TPA-An-Br** in high yield. The precursor of **TPA-An-Br** was obtained through Suzuki coupling between the commercially available chemicals of

9,10-dibromoanthracene and N,N-diphenyl-4-(4,4,5,5-tetramethyl-1,3,2-dioxaborolan-2-yl)aniline, while The AIE precursor of **TPE-BE** was prepared through the reported methods of McMurry reaction of 4-bromobenzophenone and later nucleophilic substitution. Thanks to the non-planar structure of TPE unit, the objected AIEgen of **TPA-An-TPE**, despite of its rigid structure, exhibited good solubility in common organic solvents, such as THF (tetrahydrofuran), dichloromethane and chloroform, which enabled the wet-method for structure characterization.

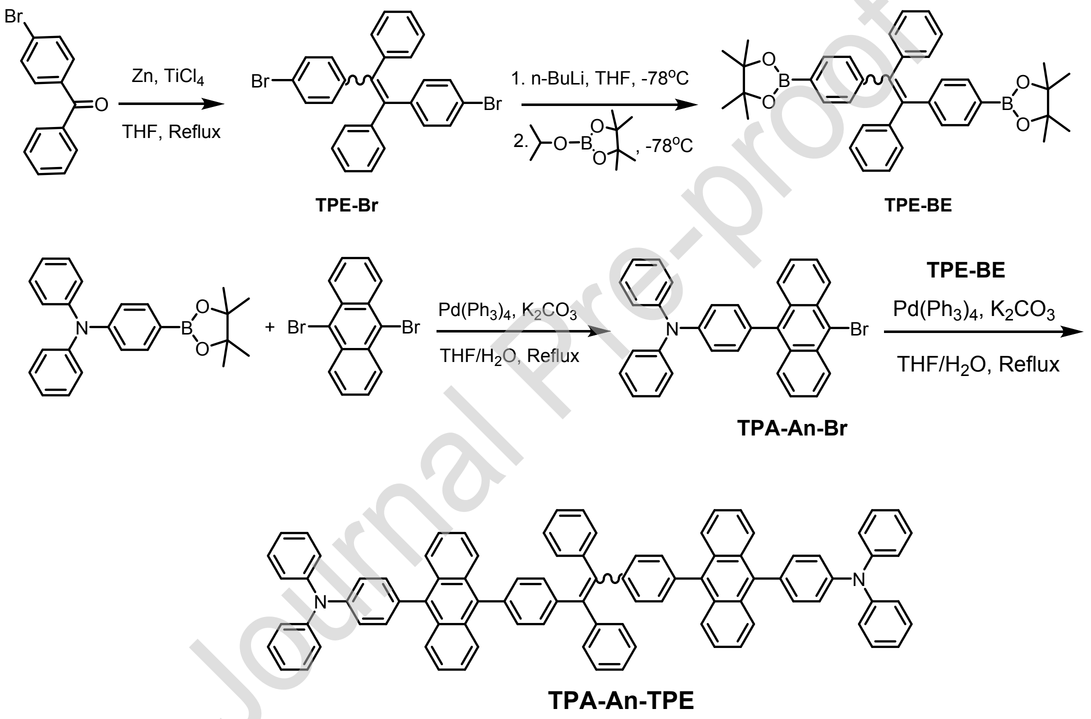

**Scheme 1**. The synthetic route to the AIEgen of **TPA-An-TPE**.

### 3.2 Thermal properties

High thermal stability is a perquisite condition for both fabrication and application of the OLED devices. Therefore, thermogravimetric analysis (TGA) and differential scanning calorimetry (DSC) were conducted on **TPA-An-TPE**. Generally, the fully aromatic components of anthracene, TPE and TPA endowed the compound with high rigidity and therefore high thermal stability. As shown in the **Figure 1**, this emitter exhibited high glass transitional temperature (Tg) of 168.3°C, high decomposition temperature of 537 °C at 5% weight loss (Td) and high mass of residual char (nearly 44%) at 800 °C, all of which indicated this compound was both thermally and morphologically stable for fabrication and application as the OLED emitters.

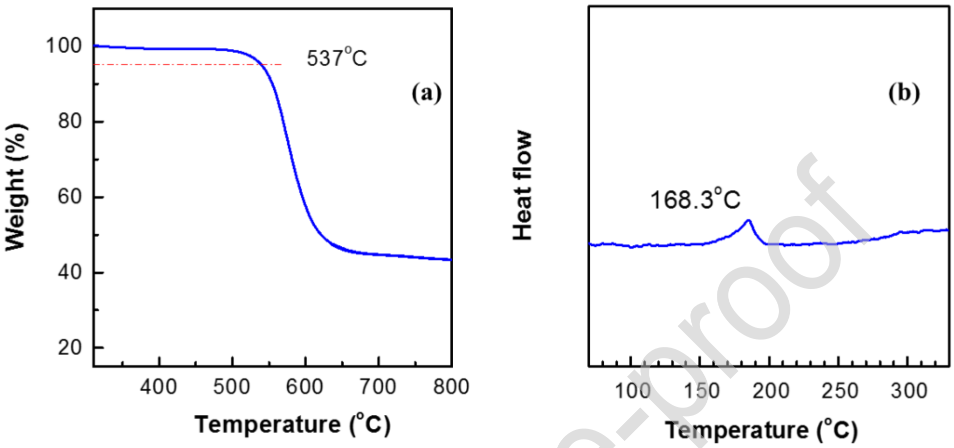

**Figure 1.** Thermogravimetric analysis (TGA) (**a**) and differential scanning calorimeter (DSC) (**b**) curves of **TPA-An-TPE**, with the scanning rate at 10 k.min$^{-1}$ under $N_2$.

### 3.3 Photophysical Properties

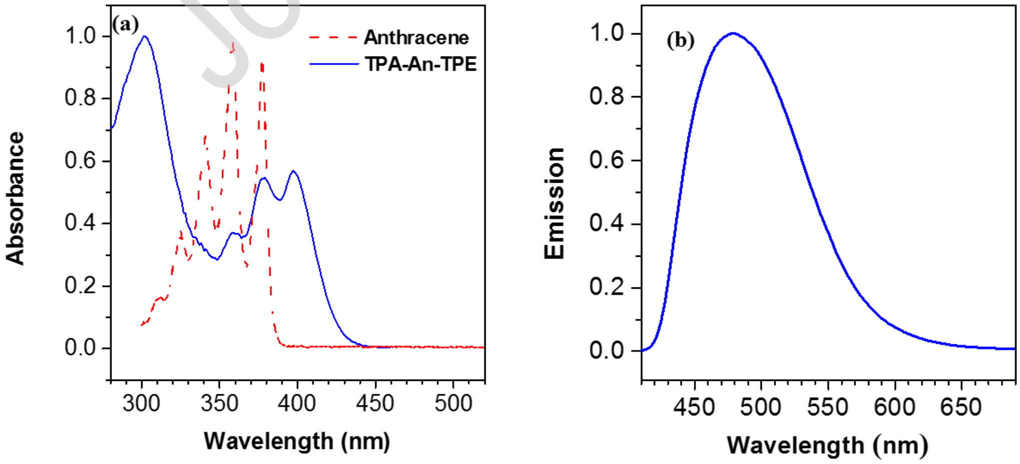

**Figure 2.** The absorbance and photoluminescence of **TPA-An-TPE** (Blue line) recorded in THF solution at the concentration of 1 mg.mL$^{-1}$.

The absorption and emission spectra of this emitter were also recorded in THF solutions are shown in **Figure 2**. The compound exhibited much fine absorption spectrum, with one peak of 398 nm quite close to the absorption peak of anthracene. The photoluminescence (PL) behaviors of **TPA-An-TPE** were also investigated in the solution and aggregated state. When dissolved into THF, the emitter of **TPA-An-TPE** exhibited weak emission with the peaks of 477 nm, because its singlet excitons tend to nonradioactive decay through vigorously intramolecular motion in good solvent as a result of its twisted conformation. Since the emitters is hydrophobic effect, their PL spectra are measured in THF/water mixtures with increasing water fractions ($f_w$) to form aggregated states (**Figure 3 a-c**). Both the intensity and the emission peak were quite complexed, which only showed the increasing tendency, but not simply monotonic increasing. However, similar phenomena were also observed and mentioned in previous research. Similarly, we also attributed the complicated PL behaviors in the mixed solvent to the formation of various kinds of nanoparticle suspensions, such as, amorphous particles and crystal particles. As for this AIEgen, water exhibited worse solubility and higher polarity compared with THF, and therefore it caused red shifted emission of the AIEgen and also an increased PL intensity with the water fraction increasing from 0% to 30%. At higher ratio of water (>30%), the aggregates appeared, which could reduce the polarity of molecular environment and therefore induce a blue shift. To be exact, from the water fraction from 40% to 70%, the amorphous aggregates appeared to decrease the PL intensity, while at the ratio of 80-90%, the water fraction would provide crystalline aggregates to increased PL intensity. However at the ratio of 99% for water, most of the AIEgens were precipitated from the solvent, and the PL intensity of the solvent have a sharp decrease.[18, 19]

Meanwhile, the powder of **TPA-An-TPE** show blue color, which exhibited strong blue emission under UV 365(**Figure 4a-b**), with the photoluminiscence quantum yield (PLQY) of 25.8%. Therefore, the emitter of **TPA-An-TPE**, thanks to the AIE-active group of TPE moiety, exhibited the AEE (aggregation-enhanced emission) nature which is much favored in the OLED devices, as most OLED emitters were applied as solid state.

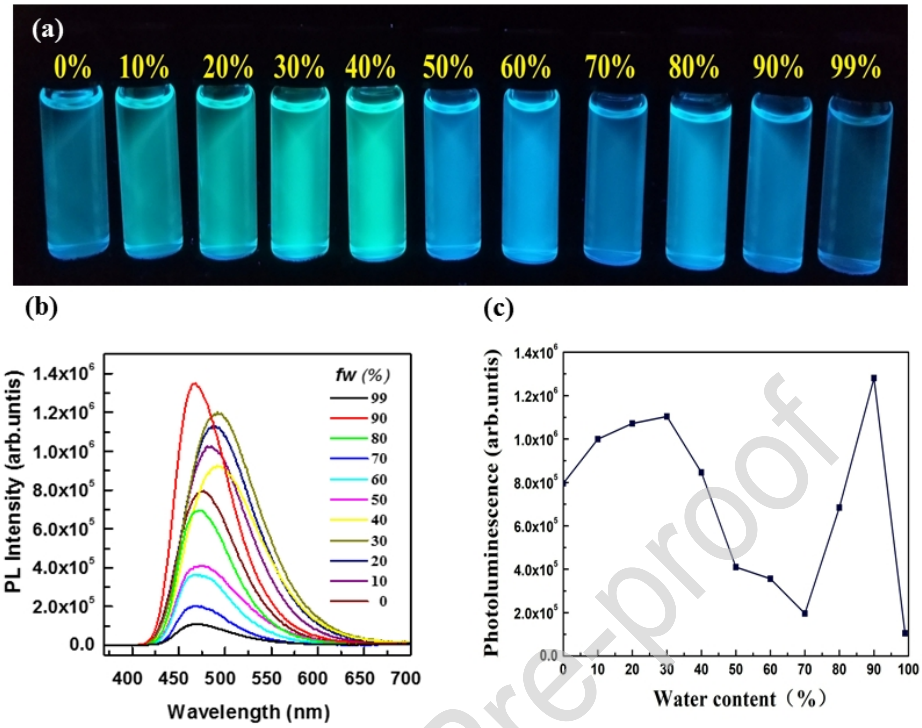

**Figure 3.** The emission photograph (a) and PL spectra (b) of **TPA-An-TPE** in THF/water mixtures, (c) and the PL intensity as a function of the ratio water fraction mixtures under 365 nm UV illumination

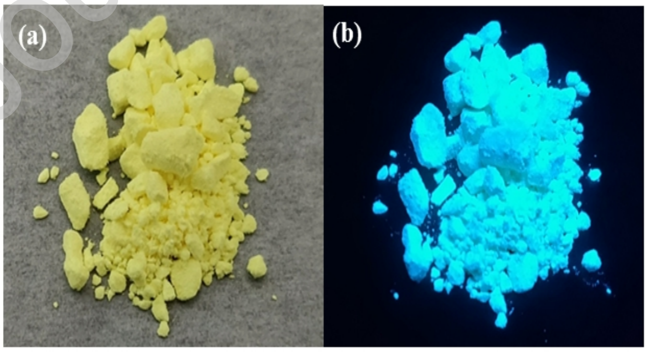

**Figure 4.** The photograph of the **TPA-An-TPE** powder under sunlight (a) and under UV light (b).

### 3.4 Theoretical calculations

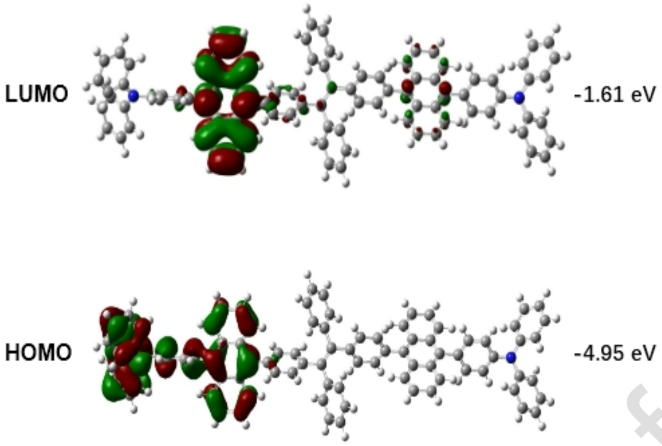

**Figure 5.** The HOMO and LUMO energy levels and distributions of **TPA-An-TPE**.

To investigate the electronic structure, density function theory (DFT) calculation was performed on **TPA-An-TPE** using the B3LYP/6-31G (d, p) set. The highest occupied molecular orbital (HOMO), lowest unoccupied molecular orbital (LUMO) and optimized geometries were displayed in **Figure 5**. This emitter adopted a quite twisted conformation between the three moieties of anthracene, TPE and TPA, with the torsional dihedral angles of 104.1$^o$ for TPA and anthracene, and 103.9$^o$ for TPE and anthracene. The HOMO and LUMO energy levels were calculated to be -4.95 eV and -1.61 eV respectively, with relatively high energy gap of 3.34 eV. The HOMO electron cloud distributions was localized on both the TPA and anthracene units, while the LUMO level was mainly localized on the anthracene core, indicating weak electronic attraction between the anthracene and TPA due to their both electron-donating properties. And the central core of TPE moiety just served as the block to link the peripheral substituents through C–C bond, but with less contribution to the HOMO and LUMO distribution.

### 3.5 Electrochemical Behaviors

In order to calculate the specific HOMO and LUMO level, the electrochemical properties of the **TPA-An-TPE** was further measured by cyclic voltammetry (CV). This AIEgen displayed onset oxidation potentials (Eox) at 0.72 eV (in **Figure 6**). Further, the HOMO energy level were calculated to be -5.12 eV, based on the equation of HOMO = - (4.4+Eox) eV[20, 21], while the LUMO energy levels are -2.22 eV from the equation of LUMO = (HOMO + Eg) eV, with Eg obtained from the on-tail absorption wavelength of 438 nm (2.90 eV). And these energy level were in accordance with the value calculated through DFT method.

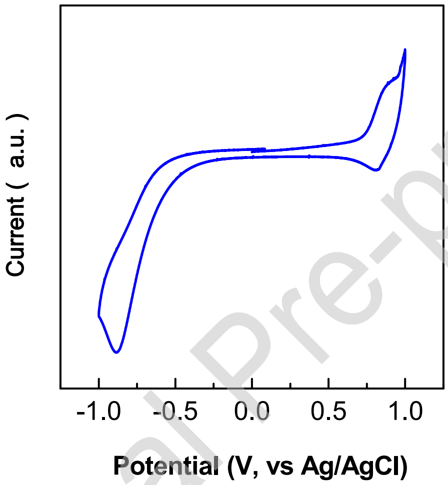

**Figure 6.** Cyclic voltammogramic behavior of TPA-An-TPE.

### 3.6 Electroluminescence

In order to evaluate the potential application of the AIEgen in OLEDs, the multilayer nondoped OLED was prepared with the architecture of indium tin oxide (ITO)/ N,N'-bis(1-naphthalenyl)-N,N'-bisphenyl-(1,1'-biphenyl)-4,4'-diamine(NPB)(40 nm)/ 4,4',4'' -tri-9-carbazolyltriphenylamine (TCTA) (5 nm)/ emitting layer (EML) (20 nm)/ 2,2',2''-(1,3,5-benzinetriyl)-tris(1-phenyl-1-*H*-benzimidazole) (TPBi) (40 nm)/ LiF (1 nm)/ Al (100 nm), where EML was fabricated merely by non-doped AIEgen

**TPA-An-TPE**, NPB and TCTA served as hole injection layer, while TPBi played the role of hole-blocking and electron transport layers, respectively. The structure and the energy-level diagram of the OLED devices were shown in **Figure. 7a**. The characterization of the EL properties of these devices is summarized in **Figure 7b-7d** and **Table 1**. It can be seen that the non-doped OLED turned on at low voltage of 3.1 eV, and radiated electroluminescence close to their PL in solid film, suggesting the exciton recombination occur in the EML layer and the EL results from the radiative decay of singlet excitons, which showed blue emission (with Full Width at Half Maximum of 100 nm), ranging from 420 to 620 nm with single peak at 474 nm, and this EL were stable from 100 to 1000 cd m$^{-2}$, confirming the emission spectrum showed minimal dependence on the current density. Unlike some emitters with the mechanism of high exciton utilization efficiency (EUE) [22-37], the OLED device based on this AIEgen experienced neither structural optimization nor out-coupling enhancement. From this angle, it is interesting to notice that the nondoped AIE emitter exhibited the maximum EQE of 2.7%. Moreover, this EQE did not see any efficiency roll-off even at 1000 cd.m$^{-2}$, which can be attributed to the fact that nonpolar AIE emitter can largely reduce quenching of emission, such as singlet–triplet and triplet–triplet annihilation.

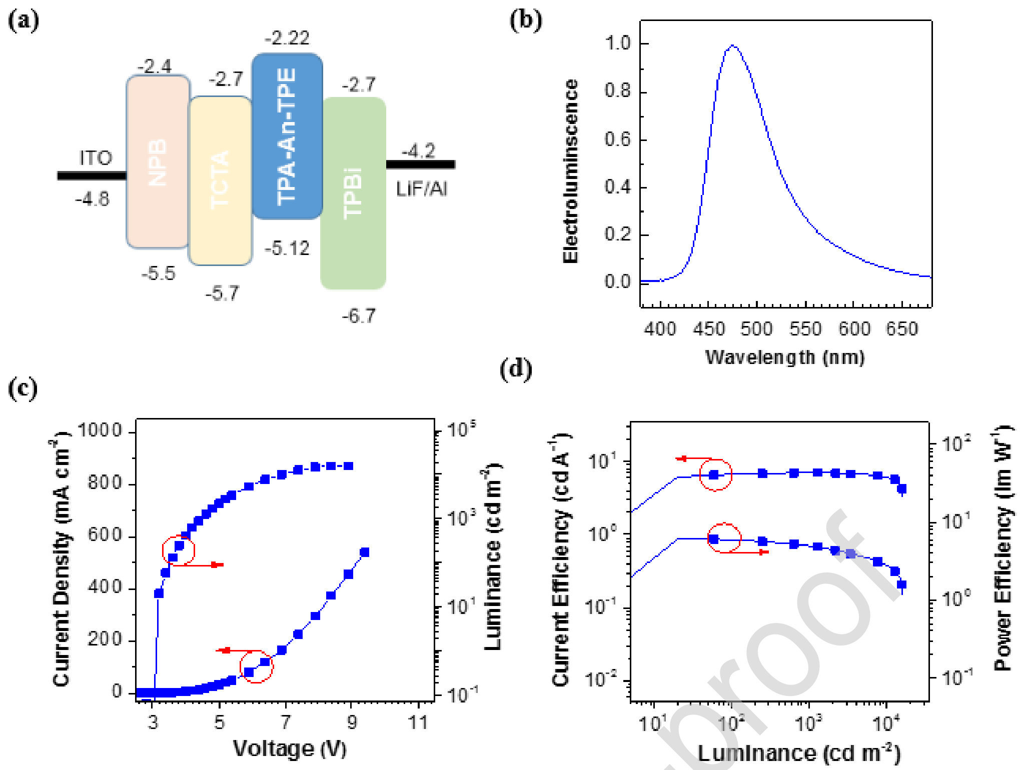

Figure 7. **(a)** Device configuration: ITO/ NPB/ TCTA/**TPA-An-TPE**/ TPBi/ LiF/ Al, **(b)** EL spectra, **(c)** changes in luminance and current density with the applied voltages, and **(d)** plots of luminance versus current efficiency and power efficiency.

**Table1.** The EL performance of non-doped blue OLED based on the emitter **TPA-An-TPE**.

| item | CE | PE | EQE | Voltage | CIE |
|---|---|---|---|---|---|
| | (cd A$^{-1}$) | (lm W$^{-1}$) | (%) | (V) | (x,y) |
| elemental data $^{a)}$ | 7.1 | 6.1 | 2.7 | 3.1 | - |
| 100 cd m$^{-2}$ | 6.7 | 5.9 | 2.7 | 3.6 | (0.18, 0.28) |
| 1000 cd m$^{-2}$ | 7.1 | 4.9 | 2.7 | 4.5 | (0.19, 0.29) |

$^{a)}$ PE: maximum power efficiency; EQE: maximum external quantum efficiency, Voltage: turn-on voltage at 1 cd m$^{-2}$.

## 4. Conclusion

In this study, a nonpolar symmetric AIEgen **TPA-An-TPE** was prepared, with TPA-ends and anthracene spacer and TPE-core. Due to its symmetric structure, this molecule **TPA-An-TPE** was prepared through quite facile steps. Thanks to its all rigid structure, **TPA-An-TPE** exhibited high Tg of 168.3 $^{o}$C and Td of 537 $^{o}$C, and the twisted structure enabled **TPA-An-TPE** to have blue photoluminescence and AEE performance, both of which were favored as OLED emitter. The blue non-doped OLED devices were therefore fabricated base on the emitter of **TPA-An-TPE**, with maximum EQE of 2.7 %, which exhibited no roll-off at1000 cd.m$^{-2}$.

## Acknowledgment

This work was financially supported by the National Key R&D Program of China (2017YFE0106000, 2016YFB0401000), National Natural Science Foundation of China (21805296, 21876158, 51773212, 21574144 and 21674123), China Postdoctoral Science Foundation (2017M621987), Zhejiang Provincial Natural Science Foundation of China (LR16B040002), Natural Science Foundation of Ningbo City (2018A610134), Ningbo Municipal Science and Technology Innovative Research Team (2015B11002 and 2016B10005), CAS Interdisciplinary Innovation Team, CAS Key Project of Frontier Science Research (QYZDB-SSW-SYS030) and CAS Key Project of International Cooperation (174433KYSB20160065).

## Contributors

Nannan Fei, Liang Cao, Honglei Ji, Yongqi Bai performed data acquirement, data analysis and wrote the manuscript; Like Huang and Ruixiang Peng helped perform the analysis with constructive discussions; Qiang Wei designed the molecule and revised the manuscript; Shiyou Hao and Ziyi Ge contributed to the conception of the study.

## References

[1] C.W. Tang, S.A. VanSlyke, Organic electroluminescent diodes, Applied Physics Letters, 51 (1987) 913-915.

[2] Q. Wei, P. Kleine, Y. Karpov, X. Qiu, H. Komber, K. Sahre, A. Kiriy, R. Lygaitis, S. Lenk, S. Reineke, B. Voit, Conjugation-Induced Thermally Activated Delayed Fluorescence (TADF): From Conventional Non-TADF Units to TADF-Active Polymers, Advanced Functional Materials, 27 (2017) 1605051.

[3] Q. Wei, R. Pötzsch, X. Liu, H. Komber, A. Kiriy, B. Voit, P.-A. Will, S. Lenk, S. Reineke, Hyperbranched Polymers with High Transparency and Inherent High Refractive Index for Application in Organic Light-Emitting Diodes, Advanced Functional Materials, 26 (2016) 2545-2553.

[4] R. Yang, Q. Guan, Z. Liu, W. Song, L. Hong, T. Lei, Q. Wei, R. Peng, X. Fan, Z. Ge, A Methodological Study on Tuning the Thermally Activated Delayed Fluorescent Performance by Molecular Constitution in Acridine–Benzophenone Derivatives, Chemistry – An Asian Journal, 13 (2018) 1187-1191.

[5] Q. Wei, Z. Ge, B. Voit, Thermally Activated Delayed Fluorescent Polymers: Structures, Properties, and Applications in OLED Devices, Macromolecular Rapid Communications, 40 (2019) 1800570.

[6] Q. Wei, N. Fei, A. Islam, T. Lei, L. Hong, R. Peng, X. Fan, L. Chen, P. Gao, Z. Ge, Small-Molecule Emitters with High Quantum Efficiency: Mechanisms, Structures, and Applications in OLED Devices, Advanced Optical Materials, 6 (2018) 1800512.

[7] X. Zhan, Z. Wu, Y. Lin, Y. Xie, Q. Peng, Q. Li, D. Ma, Z. Li, Benzene-cored AIEgens for deep-blue OLEDs: high performance without hole-transporting layers, and unexpected excellent host for orange emission as a side-effect, Chemical Science, 7 (2016) 4355-4363.

[8] X. Feng, C. Qi, H.-T. Feng, Z. Zhao, H.H.Y. Sung, I.D. Williams, R.T.K. Kwok, Jacky W.Y. Lam, A. Qin, B.Z. Tang, Dual fluorescence of tetraphenylethylene-substituted pyrenes with aggregation-induced emission characteristics for white-light emission, Chemical Science, 9 (2018) 5679-5687.

[9] B. Chen, B. Liu, J. Zeng, H. Nie, Y. Xiong, J. Zou, H. Ning, Z. Wang, Z. Zhao, B.Z. Tang, Efficient Bipolar Blue AIEgens for High-Performance Nondoped Blue OLEDs and Hybrid White OLEDs, Advanced Functional Materials, 28 (2018) 1803369.

[10] D. Ding, K. Li, B. Liu, B.Z. Tang, Bioprobes Based on AIE Fluorogens, Accounts of Chemical Research, 46 (2013) 2441-2453.

[11] J. Mei, Y.N. Hong, J.W.Y. Lam, A.J. Qin, Y.H. Tang, B.Z. Tang, Aggregation-Induced Emission: The Whole Is More Brilliant than the Parts, Advanced Materials, 26 (2014) 5429-5479.

[12] F. Liu, Y. Tao, J. Li, H. Liu, X. He, C. Du, X. Tang, P. Lu, Efficient Non-doped Blue Fluorescent Organic Light-Emitting Diodes Based on Anthracene–Triphenylethylene Derivatives, Chemistry – An Asian Journal, 14 (2019) 1004-1012.

[13] P. Bhui, Q.T. Siddiqui, M. Muneer, N. Agarwal, S. Bose, Deep blue organic light-emitting diodes of 1,8-diaryl anthracene, J. Chem. Sci., 130 (2018) 9.

[14] H.J. Yen, G.S. Liou, Recent advances in triphenylamine-based electrochromic derivatives and polymers, Polymer Chemistry, 9 (2018) 3001-3018.

[15] H.J. Yen, G.S. Liou, Design and preparation of triphenylamine-based polymeric materials towards emergent optoelectronic applications, Progress in Polymer Science, 89 (2019) 250-287.

[16] M.H. Chua, Q. Zhu, K.W. Shah, J.W. Xu, Electroluminochromic Materials: From Molecules to Polymers, Polymers, 11 (2019) 35.

[17] W. Wu, S. Ye, L. Huang, L. Xiao, Y. Fu, Q. Huang, G. Yu, Y. Liu, J. Qin, Q. Li, Z. Li, A conjugated hyperbranched polymer constructed from carbazole and tetraphenylethylene moieties: convenient synthesis through one-pot “A2 + B4” Suzuki polymerization, aggregation-induced enhanced emission, and application as explosive chemosensors and PLEDs, Journal of Materials Chemistry, 22 (2012) 6374-6382.

[18] X. Zhang, Z. Chi, B. Xu, C. Chen, X. Zhou, Y. Zhang, S. Liu, J. Xu, End-group effects of piezofluorochromic aggregation-induced enhanced emission compounds containing distyrylanthracene, Journal of Materials Chemistry, 22 (2012) 18505-18513.

[19] X. Zhang, Z. Ma, Y. Yang, X. Zhang, Z. Chi, S. Liu, J. Xu, X. Jia, Y. Wei, Influence of alkyl length on properties of piezofluorochromic aggregation induced emission compounds derived from 9,10-bis[(N-alkylphenothiazin-3-yl)vinyl]anthracene, Tetrahedron, 70 (2014) 924-929.

[20] H. Shi, S. Wang, L. Qin, C. Gui, X. Zhang, L. Fang, S. Chen, B.Z. Tang, Construction of two AIE luminogens comprised of a tetra-/tri-phenylethene core and carbazole units for non-doped organic light-emitting diodes, Dyes and Pigments, 149 (2018) 323-330.

[21] S. Chen, X. Xu, Y. Liu, G. Yu, X. Sun, W. Qiu, Y. Ma, D. Zhu, Synthesis and Characterization of n‐Type Materials for Non‐Doped Organic Red‐Light‐Emitting Diodes, Advanced functional materials, 15 (2005) 1541-1546.

[22] D.X. Ma, T. Tsuboi, Y. Qiu, L. Duan, Recent Progress in Ionic Iridium(III) Complexes for Organic Electronic Devices, Advanced Materials, 29 (2017) 33.

[23] A.J. Huckaba, M.K. Nazeeruddin, Strategies for Tuning Emission Energy in Phosphorescent Ir(III) Complexes, Comments on Inorganic Chemistry, 37 (2017) 117-145.

[24] A.B. Tamayo, S. Garon, T. Sajoto, P.I. Djurovich, I.M. Tsyba, R. Bau, M.E. Thompson, Cationic Bis-cyclometalated Iridium(III) Diimine Complexes and Their Use in Efficient Blue, Green, and Red Electroluminescent Devices, Inorganic Chemistry, 44 (2005) 8723-8732.

[25] H. Xu, R. Chen, Q. Sun, W. Lai, Q. Su, W. Huang, X. Liu, Recent progress in metal-organic complexes for optoelectronic applications, Chemical Society Reviews, 43 (2014) 3259-3302.

[26] J. Lee, H.-F. Chen, T. Batagoda, C. Coburn, P.I. Djurovich, M.E. Thompson, S.R.

Forrest, Deep blue phosphorescent organic light-emitting diodes with very high brightness and efficiency, Nature Materials, 15 (2015) 92.

[27] A. Endo, M. Ogasawara, A. Takahashi, D. Yokoyama, Y. Kato, C. Adachi, Thermally Activated Delayed Fluorescence from Sn4+–Porphyrin Complexes and Their Application to Organic Light Emitting Diodes — A Novel Mechanism for Electroluminescence, Advanced Materials, 21 (2009) 4802-4806.

[28] H. Uoyama, K. Goushi, K. Shizu, H. Nomura, C. Adachi, Highly efficient organic light-emitting diodes from delayed fluorescence, Nature, 492 (2012) 234-238.

[29] A. Chihaya, Third-generation organic electroluminescence materials, Japanese Journal of Applied Physics, 53 (2014) 060101.

[30] Z. Yang, Z. Mao, Z. Xie, Y. Zhang, S. Liu, J. Zhao, J. Xu, Z. Chi, M.P. Aldred, Recent advances in organic thermally activated delayed fluorescence materials, Chemical Society Reviews, 46 (2017) 915-1016.

[31] J.-Y. Hu, Y.-J. Pu, F. Satoh, S. Kawata, H. Katagiri, H. Sasabe, J. Kido, Bisanthracene-Based Donor–Acceptor-type Light-Emitting Dopants: Highly Efficient Deep-Blue Emission in Organic Light-Emitting Devices, Advanced Functional Materials, 24 (2014) 2064-2071.

[32] S.J. Cha, N.S. Han, J.K. Song, S.-R. Park, Y.M. Jeon, M.C. Suh, Efficient deep blue fluorescent emitter showing high external quantum efficiency, Dyes and Pigments, 120 (2015) 200-207.

[33] N.A. Kukhta, T. Matulaitis, D. Volyniuk, K. Ivaniuk, P. Turyk, P. Stakhira, J.V. Grazulevicius, A.P. Monkman, Deep-Blue High-Efficiency TTA OLED Using Para- and Meta-Conjugated Cyanotriphenylbenzene and Carbazole Derivatives as Emitter and Host, The Journal of Physical Chemistry Letters, 8 (2017) 6199-6205.

[34] W. Li, D. Liu, F. Shen, D. Ma, Z. Wang, T. Feng, Y. Xu, B. Yang, Y. Ma, A Twisting Donor-Acceptor Molecule with an Intercrossed Excited State for Highly Efficient, Deep-Blue Electroluminescence, Advanced Functional Materials, 22 (2012) 2797-2803.

[35] S. Zhang, W. Li, L. Yao, Y. Pan, F. Shen, R. Xiao, B. Yang, Y. Ma, Enhanced proportion of radiative excitons in non-doped electro-fluorescence generated from an imidazole derivative with an orthogonal donor-acceptor structure, Chemical Communications, 49 (2013) 11302-11304.

[36] W. Li, Y. Pan, R. Xiao, Q. Peng, S. Zhang, D. Ma, F. Li, F. Shen, Y. Wang, B. Yang, Y. Ma, Employing ∼100% Excitons in OLEDs by Utilizing a Fluorescent Molecule with Hybridized Local and Charge-Transfer Excited State, Advanced Functional Materials, 24 (2014) 1609-1614.

[37] L. Yao, S. Zhang, R. Wang, W. Li, F. Shen, B. Yang, Y. Ma, Highly Efficient Near-Infrared Organic Light-Emitting Diode Based on a Butterfly-Shaped Donor–Acceptor Chromophore with Strong Solid-State Fluorescence and a Large Proportion of Radiative Excitons, Angewandte Chemie International Edition, 53 (2014) 2119-2123.

# Highlights

- This emitter with good thermal stability and aggregation-enhanced emission (AEE) characteristics
- non-doped blue OLED device was fabricated with the maximum external quantum efficiency (EQE) of 2.7%.
- non-doped blue OLED device with no efficiency roll-off even at 1000 cd.m$^{-2}$.

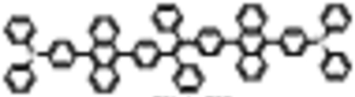

TPA-An-TPE


-2.22
-2.4
-2.7
-2.7
ITO
-4.8
NPB
TCTA
TPA-An-TPE
TPBi
-4.2
LiF/Al
-5.12
-5.5
-5.7
-6.2

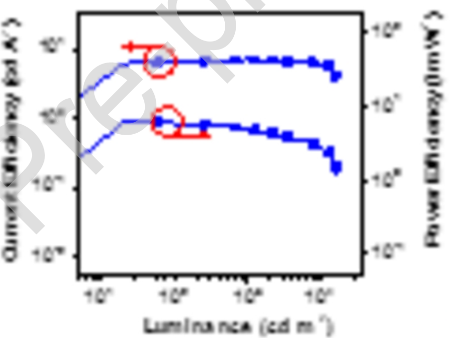
Current Efficiency (cd A$^{-1}$)
Power Efficiency (lm W$^{-1}$)
$10^{1}$
$10^{0}$
$10^{-1}$
$10^{-2}$
Luminance (cd m$^{-2}$)